Available online at www.sciencedirect.com
SCIENCE DIRECT®
Journal of Theoretical Biology 223 (2003) 283–298
Journal of Theoretical Biology
www.elsevier.com/locate/jtbi

Oscillations in cyclical neutropenia: new evidence based on mathematical modeling

Samuel Bernard[a,1], Jacques Bélair[a,b,2], Michael C. Mackey[c,*,3]

[a] *Département de Mathématiques et de Statistique and Centre de recherches mathématiques, Université de Montréal, C.P. 6128, Succ. Centre-Ville, Montréal, Qué., Canada H3C 3J7*
[b] *Centre for Nonlinear Dynamics, McGill University, Canada*
[c] *Departments of Physiology, Physics and Mathematics and Centre for Nonlinear Dynamics, McGill University, 3655 Drummond, Montréal, Qué., Canada H3G 1Y6*

Received 25 February 2002; received in revised form 7 February 2003; accepted 19 February 2003

Abstract

We present a dynamical model of the production and regulation of circulating blood neutrophil number. This model is derived from physiologically relevant features of the hematopoietic system, and is analysed using both analytic and numerical methods. Supercritical Hopf bifurcations and saddle-node bifurcations of limit cycles are shown to exist. We make the estimation of kinetic parameters for dogs and then apply the model to cyclical neutropenia (CN) in the grey collie, a rare disorder in which oscillations in all blood cell counts are found. We conclude that the major cause of the oscillations in CN is an increased rate of apoptosis of neutrophil precursors which leads to a destabilization of the hematopoietic stem cell compartment.

Keywords: Cyclical neutropenia; Hopf bifurcation; Delay differential system; Hematopoiesis; Stem cell model

1. Introduction

Hematopoiesis is the term used to describe the production of blood cells. Even though all blood cells come from a unique source, the hematopoietic stem cells (HSC), the mechanisms regulating this production are still obscure. Nevertheless, it seems clear that the production of erythrocytes and platelets is controlled by feedback mechanisms involving specific cytokines such as erythropoietin (Epo) and thrombopoietin (Tpo) (Haurie et al., 1998; Mahaffy et al., 1998; Santillan et al., 2000). However, the regulation of leukopoiesis (production of white blood cells) is not as well understood and the local HSC regulation mechanisms are even less clear (Rubinow and Lebowitz, 1975; MacDonald, 1978; Hearn et al., 1998; Haurie et al., 1998, 1999a, b, 2000; Mackey, 2001). Because of their dynamical character, cyclical neutropenia (CN) and other periodic hematological disorders offer us opportunities to better comprehend the nature of these regulatory processes (von Schulthess and Mazer, 1982).

CN is a rare hematological disorder characterized by oscillations in the circulating neutrophil count. These levels fall from normal to barely detectable levels with a period of 19–21 days in humans (Guerry et al., 1973; Dale and Hammond, 1988; Haurie et al., 1998), and periods up to 40 days have been observed (Haurie et al., 1998). These oscillations in the neutrophil count about a subnormal level are generally accompanied by oscillations around normal levels in other blood cell lineages such as platelets, lymphocytes and reticulocytes (Haurie et al., 1998, 2000).

*Corresponding author.
E-mail addresses: bernard@dms.umontreal.ca (S. Bernard), belair@crm.umontreal.ca (J. Bélair), mackey@cnd.mcgill.ca (M.C. Mackey).
[1] SB is supported by MITACS (Canada) and ISM (Québec).
[2] JB is supported by the Natural Sciences and Engineering Research Council (NSERC Grant No. OGP-0008806, Canada), MITACS (Canada) and Le Fonds pour la Formation de Chercheurs et l'Aide à la Recherche (FCAR Grant No. 98ER1057, Québec).
[3] MCM is supported by the Natural Sciences and Engineering Research Council (NSERC Grant No. OGP-0036920, Canada), MITACS (Canada), the Alexander von Humboldt Stiftung, and Le Fonds pour la Formation de Chercheurs et l'Aide à la Recherche (FCAR Grant No. 98ER1057, Québec).

0022-5193/03/$ - see front matter
doi:10.1016/S0022-5193(03)00090-0

Many mathematical models have been proposed to explain the origin of these oscillations as well as to understand the control of neutrophil production in non-pathological cases. For a discussion of previous models that have been developed see, Hearn et al. (1998). In most of them, the production is controlled by a feedback loop located at the level of the neutrophil precursors. Many authors have suggested a destabilization of this feedback loop as a source of oscillations in the neutrophil count seen in CN (Morley et al., 1969; Morley and Stohlman, 1970; Morley, 1970; King-Smith and Morley, 1970; Reeve, 1973; MacDonald, 1978; Kazarinoff and van den Driessche, 1979; von Schulthess and Mazer, 1982; Shvitra et al., 1983; Wichmann et al., 1988; Schmitz et al., 1990, 1995). However, it has also been shown to be unlikely that such a destabilization could account for oscillations in CN (Hearn et al., 1998), further suggesting that the origin of the oscillations is due to destabilization of the HSC regulation mechanisms. This would also explain the fact that other cell lineages oscillate with the same period as the neutrophils (Haurie et al., 1998, 2000).

Fortunately, CN is found in an animal model. All grey collies (Lund et al., 1967) are born with this congenital disease with an oscillation period on the order of 11–16 days (Haurie et al., 1998, 1999b, 2000). This canine model has provided extensive experimental data on the nature of CN. The challenge is to transfer to humans the knowledge derived from dogs.

In this paper, our primary goal is to model CN in the grey collie and understand its dynamic behaviour. A variety of experimental data show that CN is associated with an elevated rate of apoptosis in neutrophil precursors (Dale et al., 2000; Aprikyan et al., 2001). The model developed in this paper is used to explore the possibility that the oscillations characteristic of CN are actually a consequence of this increased rate of apoptosis.

The paper is organized as follow. In Section 2 we develop the model, which is a simple two-compartment production system. In Section 3, we use the experimental and clinical literature to estimate the model parameters, mainly using data from mice and dogs. In Section 4 we analyse the model using a combination of analytical and numerical continuation methods. A local supercritical Hopf bifurcation and a saddle-node bifurcation of limit cycles are found as critical parameters are varied. Numerical simulations are presented in Section 5. In Section 6 we present a new hypothesis for the origin of the oscillations characteristic of CN. We propose this oscillation mechanism as a generic way to introduce oscillations in hematopoiesis. In Section 7, we discuss some of the difficulties in estimating the system parameters for dogs and the important issues in adapting such a model for humans.

2. A model of white blood cell production

2.1. The model equations

Fig. 1 illustrates the two components of this model: the hematopoietic stem cell (HSC) compartment (denoted S) and the maturing neutrophil compartment (denoted N). The HSCs are self-renewing and pluripotential (can differentiate into any blood cell type), and the rate at which they differentiate into the neutrophil line is assumed to be determined by the level of circulating neutrophils. As these neutrophil precursors differentiate, their numbers are amplified by successive divisions. After a certain maturation time τ_N they become mature neutrophils and are released into blood. The transit time through the neutrophil precursor compartment is not fixed but follows a distribution of times resembling a gamma distribution (Guerry et al., 1973; Deubelbeiss et al., 1975; Price et al., 1996; Basu et al., 2002). In the present paper however, the single fixed transit time τ_N will be used since it simplifies the model without compromising essential features (Bernard et al., 2001).

As shown in Fig. 1, there are two feedback loops. The first is between the mature neutrophil compartment and the rate ($F(N)$) of HSC differentiation into the neutrophil line. $F(N)$ operates with a delay τ_N that

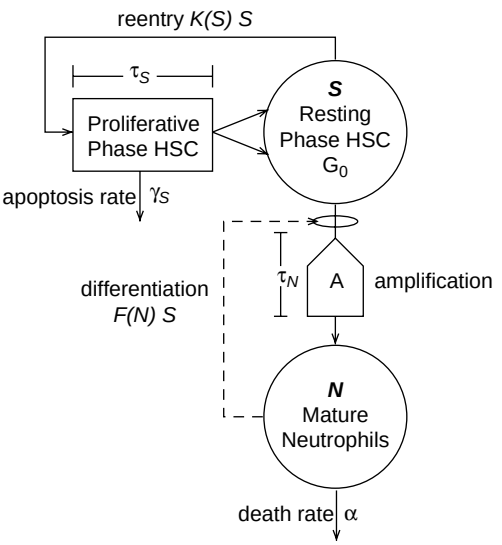

Fig. 1. Model of neutrophil production. The variable S represents the number of HSC in the resting (G_0) phase. Cells in the resting phase can either enter the proliferative phase at a rate $K(S)$ or differentiate at a rate $F(N)$ to ultimately give rise to mature neutrophils N, the second variable. Cells in the HSC proliferative phase undergo apoptosis at a rate γ_S and the cell cycle duration is τ_S. Cells in the differentiation pathway are amplified by successive divisions by a factor A which is also used to account for cell loss due to apoptosis. After a time τ_N, differentiated cells become mature neutrophils N and are released into the blood. It is assumed that mature neutrophils die at a fixed rate α. Two feedback loops control the entire process through the proliferation rate $K(S)$ and the differentiation rate $F(N)$.

accounts for the time required for neutrophil division and maturation so the flux of cells from the resting phase of the HSC compartment is $F(N\tau_N)S\tau_N$. Here, as elsewhere, the notation x_τ means $x(t-\tau)$.

The second loop regulates the rate ($K(S)$) at which HSCs reenter the proliferative cycle from G_0 state, and it operates with a delay τ_S that accounts for the length of time required to produce two daughter HSCs from one mother cell. $K(S)$ is a monotone decreasing function of S (and therefore acts like a negative feedback). The flux of cells out of the resting phase of the HSC compartment is given by $K(S)S$. $K(S)$ regulates the level of hematopoietic stem cells (S), while $F(N)$ controls the number of neutrophils.

The main agent controlling the peripheral neutrophil regulatory system through $F(N)$ is granulocyte colony stimulating factor (G-CSF), which acts in two ways. First, it decreases the apoptosis rate of neutrophil precursors (leading to an increase of the amplification number A in the model (Basu et al., 2002) and, second, it increases the rate of HSC differentiation into the neutrophil precursor compartment. The clearance of G-CSF decreases as the number of neutrophils decreases (Kearns et al., 1993; Terashi et al., 1999) and the neutrophil count increases when the level of G-CSF is increased (Petros, 1992; Chatta et al., 1994; Price et al., 1996). This type of regulation suggests a negative feedback: an increase of neutrophil count is followed by a decrease in G-CSF concentration, leading to a decrease in neutrophil count. The effect of G-CSF is analysed in Appendix A. Other effects of elevated G-CSF concentration are to decrease both the mean and variance of the maturation time τ_N (Chatta et al., 1994; Schmitz et al., 1994; Price et al., 1996; Haurie et al., 1999b) and to decrease the rate of apoptosis of stem cells.

In the present model, we have implicitly included the effect of G-CSF through the feedback $F(N)$. We have not included the effect of G-CSF on the amplification A. Rather, the parameter A is used as a bifurcation parameter. A recent study indicates that CN is associated, in part, with an increased rate of apoptosis (Aprikyan et al., 2001) and the model developed and analysed in this paper is used to determine whether this effect is sufficient to induce the dynamical behaviour of the neutrophil count observed in CN.

From Fig. 1 we can write down the model equations. The production of N is equal to the influx $F(N)S$ in the precursor compartment times the amplification A, delayed by the transit time τ_N, for a total production of $AF(N_{\tau_N})S_{\tau_N}$. The loss from the compartment N is the efflux to death αN, so that the total variation of N is

$$\frac{dN}{dt} = -\alpha N + AF(N_{\tau_N})S_{\tau_N}. \quad (1)$$

The production of S is equal to the flux of cells reentering the proliferative phase, $K(S)S$, times the fraction of surviving cells $\exp(-\gamma_S\tau_S)$ times the cell division factor 2, delayed by the cell cycle time τ_S, for a total production of $2\exp(-\gamma_S\tau_S)K(S\tau_S)S\tau_S$. The loss from compartment S is the flux reentering the proliferating phase, $K(S)S$, plus the efflux into differentiation $F(N)S$.

The total variation of S is then

$$\frac{dS}{dt} = -F(N)S - K(S)S + 2e^{-\gamma_s\tau_S}K(S_{\tau_s})S_{\tau_s}. \quad (2)$$

The model parameters are the circulating neutrophil death rate α, the neutrophil pathway amplification A, the maturation delay of neutrophil precursor τ_N, the HSC proliferative phase duration τ_S and the apoptotic rate of proliferating HSC, γ_S. As noted above, the function F is the differentiation rate from the HSC compartment into the neutrophil lineage and the function K is the HSC self-renewal (proliferation) rate. These functions are made more precise in Appendix A.

3. Parameter estimation

Estimation of the parameters is one of the most critical aspects of our work since it is crucial to establish the cause for the onset of oscillations in CN. Parameters that are outside the feedback functions can be retrieved or easily derived from experimental data found in literature.

In humans and dogs, circulating neutrophils disappear at a rate of $\alpha = 2.4\,\text{day}^{-1}$ (Deubelbeiss et al., 1975; Haurie et al., 2000). A number of these parameters depend on the number of stem cells S at steady state. Estimates of this number can vary dramatically, depending on what kind of cells are classified as stem cells. Here a stem cell is defined as a non-differentiated, pluripotential and self-renewing cell. Data from the literature (Boggs et al., 1982; Micklem et al., 1987; Harrison et al., 1988; McCarthy, 1997) give a value of between 1 and 50 stem cells per 10^5 nucleated bone marrow cells in mice with a value of 8 stem cells per 10^5 nucleated bone marrow cells in cats (Abkowitz et al., 2000). Novak and Nečas (1994) give a mean count of 1.4×10^{10} nucleated bone marrow cells per kg in mice. This leads to an estimate of 1.12×10^6 HSC/kg.[4] We assume a number of stem cells of $S_* = 1.1\times10^6$ cell/kg of body weight. The daily neutrophil production in dogs has been evaluated to 1.65×10^9 cell/kg/day (Deubelbeiss et al., 1975). The average circulating neutrophil count N_* is therefore 6.9×10^8 cells/kg. The

[4] The actual density of HSC in the bone marrow is almost immaterial. Indeed, changing the HSC level by a factor 10 together with the amplification A will result in the same values. Therefore, we will use the value 1.12×10^6 HSC/kg for the normal HSC number.

proliferation rate K has been evaluated for mice in Abkowitz et al. (2000) to be about 20–25 times per year and once each 19 days in Bradford et al. (1997), giving a value of $K_* = 0.06\,\text{day}^{-1}$. Under steady-state assumption, with an apoptosis rate into the HSC proliferative phase $\gamma_S = 0.07\,\text{day}^{-1}$ (Mackey, 2001), and a cell cycle duration $\tau_S = 2.8$ days (Mackey, 2001; Cheshier et al., 1999; Abkowitz et al., 2000), we find

$$F_* = \frac{K_*}{2e^{-\gamma_S T_S} - 1} = 0.04\,\text{day}^{-1}. \quad (3)$$

Then, we can give an estimation of the normal amplification factor between HSCs and the mature neutrophil pool

$$A = \frac{\alpha N_*}{F_* S_*} = 2^{15.2}. \quad (4)$$

This is the effective amplification, and without apoptosis in the proliferative compartment of neutrophil precursors, the number of divisions performed by precursors would be around 15. The ratio between the steady-state granulocyte turnover rate (GTR) and the maximal turnover rate (when there is no apoptosis) has been estimated as between 8 and 16 (Hearn et al., 1998; Haurie et al., 2000), implying that 3 or 4 more divisions than the effective number of division is required to produce enough neutrophil under steady state. The maximum total number of divisions between the stem cell and mature neutrophils is then around 18 (15 effective plus 3 to compensate apoptosis).

The parameters within the feedback functions $K(S)$ and $F(N)$ are much more difficult to estimate. Under steady-state conditions, these functions are constant, so we must rely on the dynamics of CN to guide these estimations. Since the dynamics found in CN are varied (Haurie et al., 1998, 1999b), we may expect an equally large variation in these parameters.

The two feedback functions include six parameters: f_0, k_0, θ_1, θ_2, n, and s. These parameters have been fitted by visual inspection of the dynamics of the model compared to experimental data on circulating neutrophil counts in CN. However, some of these parameters can be related to other experimental data or modeling. The maximal reentry rate k_0 can be evaluated from cell division tracking experiments (Lyons, 1999). In a recent study (Bernard et al., in review), a model based on physiologically relevant properties was used to evaluate kinetic parameters from primitive murine bone marrow cells stimulated in vitro (Oostendorp et al., 2000). Values of 2.0–2.5 day^{-1} were found for the reentry rate into the cell cycle, suggesting a value of $k_0 \geqslant 2.5\,\text{day}^{-1}$. A value of $k_0 = 8.0\,\text{day}^{-1}$ gave a good fit to experimental data. The parameter s controls the steepness of the feedback function K, and is associated with the number of cytokines involved in the division signaling (see Appendix A). It is not clear what this value should be but there is evidence that at least two different cytokines are needed to trigger HSC proliferation in vitro (Mckinstry et al., 1997). In (Pujo-Menjouet and Mackey, to appear), a study is carried out when s takes large values, but traditionally small values have been used in modeling (Andersen and Mackey, 2001). We will therefore assume a value of $s = 2$. The two parameters k_0 and s, with the steady-state value K_* allow us to compute the value of $\theta_2 = 0.095 \times 10^6$ cell/kg. With the same argument, we will choose $n = 1$, since we are primarily concerned with the effect of G-CSF alone.

The parameters of F, f_0 and θ_1, are more difficult to estimate since cellular differentiation dynamics are not well characterized. Some experiments report a 20-fold increase in differentiation activity under administration of G-CSF (Lotem and Sachs, 1988; Ward et al., 1999; Akbarzadeh et al., 2002) suggesting a value of f_0 of the order of $20 \times 0.04 = 0.8\,\text{day}^{-1}$. This value, along with F_* and n, gives a value of $\theta_1 = 0.36 \times 10^8$ cell/kg.

Table 1 shows the ranges for which the parameters are in agreement with experimental data.

Table 1
Estimated model parameters

Parameter	Unit	Range	Value used	Reference
A	100	0–1000	380	1, 2
f_0	day^{-1}	0.4–1.5	0.8	3, m
θ_1	10^8 cell/kg	0.1–2.0	0.36	m
k_0	day^{-1}	2.0–10.0	8.0	m
θ_2	10^6 cell/kg	0.0001–0.10	0.095	m
n	—	—	1	4
s	—	2–3	2	4
τ_N	day	3.0–10	3.5	5
τ_S	day	1.4–4.2	2.8	1, 6
γ_S	day	0.01–0.20	0.07	1
α	day^{-1}	2.2–2.5	2.4	7
S_*	10^6 cell/kg	0.001–1.1	1.1	1, 8
N_*	10^8 cell/kg	5.0–10	6.9	1, 9
F_*	day^{-1}	0.01–0.04	0.04	1
K_*	day^{-1}	0.02–0.06	0.06	1

The "range" column shows values found in literature or values, which are consistent with numerical simulation. The column "value used" shows the value used here in the numerical analysis and simulations. For the references, 1 = (Mackey, 2001), 2 = (Novak and Nečas, 1994; Hearn et al., 1998), 3 = (Haurie et al., 2000), 4 = (Andersen and Mackey, 2001; Niu et al., 1999; Bagley et al., 1997), 5 = (Lebowitz and Rubinow, 1969; Nakamura, 1999; Burthem et al., unpublished), 6 = (Cheshier et al., 1999), 7 = (Haurie et al., 2000, 1999b; Hearn et al., 1998), 8 = (Edelstein-Keshet et al., 2001), 9 = (Haurie et al., 2000). The "m" in reference means that the parameter has been chosen to make the model fit available data. All HSC data come from mice, cats, or dogs.

4. Analysis of the model

4.1. Two mechanisms for the onset of oscillations

In this section we study the linear stability of the model Eqs. (1) and (2). First note that there exists one and only one positive steady state for N and S if

$$f_0 < \tfrac{1}{2}(2\exp(-\gamma_S\tau_S) - 1)k_0 \tag{5}$$

(see Appendix B for a proof of this claim). The right-hand side of this equation is half the output of the HSC proliferative phase minus one, i.e. half the net increase due to one cell division times the proliferative rate k_0. The condition states that the rate of differentiation must be smaller than this output rate. Condition (5) is always satisfied for the range of parameters used here. Let N_* and S_* denote the unique positive steady-state values of N and S, respectively, when it exists. Then in the neighbourhood of this unique non-trivial stationary solution, we can linearize Eqs. (1) and (2) to obtain the characteristic equation

$$\begin{aligned}\lambda^2 &- (A_1 + B_2)\lambda - A_2\lambda e^{-\lambda\tau_N} - B_3\lambda e^{-\lambda\tau_S} + B_2A_1\\ &+ (A_2B_2 + B_1A_3)e^{-\lambda\tau_N} + A_1B_3e^{-\lambda\tau_S}\\ &+ A_2B_3e^{-\lambda(\tau_N+\tau_S)} = 0.\end{aligned} \tag{6}$$

This characteristic equations is derived in Appendix C. Eq. (6) is a transcendental equation and it is not possible to study the roots of this equation by means of analytical tools alone. A simpler equation is obtained, however, if we assume that the function F is a constant. In that case, Eq. (2) is uncoupled from Eq. (1) and an analytical stability study can be performed on Eq. (2) alone. The mechanisms leading to oscillations found in this simpler reduction of the model have been also found numerically in the full nonlinear model, i.e. when F is a function of the number of neutrophils N. These mechanisms are explained below and numerical methods have been used to plot the bifurcation diagrams for the full model (Figs. 3 and 4).

Based on our model analysis, there are two physiologically plausible mechanisms that can lead to oscillation in the model described by Eqs. (1) and (2). Both involve the stem cell compartment:

Mechanism 1. In the first, we assume that the stem cell parameters are at their normal values (cf. Table 1), and we mimic an increase in the rate of apoptosis in the neutrophil compartment by decreasing the parameter A. This leads to an increase in the stem cell differentiation rate $F(N)$ that may destabilize the stem cell compartment.

Mechanism 2. The other mechanism is an increase in the apoptosis rate γ_S in the stem cell compartment. This leads to an increased rate of replication $K(S)$ that may also destabilize the system. The second mechanism has been studied in (Mackey, 1978; Fowler and Mackey, 2002), and can lead to long period oscillations (from 20 to 40 days, as shown in Fig. 5, bottom panel). This destabilization can only occur when the differentiation rate F is sufficiently small.[5]

To distinguish between the two mechanisms, we have to look at the sign of B_2 in Eq. (6). If B_2 is positive, then a long period (greater than $4\tau_S$) bifurcation can occur. A high value of F in B_2 will make it negative and in this case an increase in γ_S will give the same effect as Mechanism 1. Let $F = F_*$ be constant, so that A_2 and B_1 are zero. This is the quasi-steady-state assumption. The characteristic equation (6) reduces to

$$(\lambda - A_1)(\lambda - B_2 - B_3\exp(-\lambda\tau_S)) = 0. \tag{7}$$

As long as $A_1 < 0$, the stability only depends on the second factor in Eq. (7). The location of the roots of Eq. (7) will determine the stability of Eqs. (1) and (2) under the quasi-steady-state assumption. This characteristic equation (7) has been studied in many papers and recently in Bernard et al. (2001). The stability space (B_1, B_2) can be divided in three regions.

(1) If $-B_2 \geqslant |B_3|$, then the steady state of system (1, 2) is locally stable;
(2) if $B_3 > -B_2$, then the unique positive steady-state condition is violated, and we will not consider this case further;
(3) if $B_3 \leqslant -|B_2|$, then the local stability of system (1, 2) is dependent on the following condition (Hayes, 1950):

$$\tau_S < \frac{\operatorname{across}(-B_2/B_3)}{\sqrt{B_3^2 - B_2^2}}. \tag{8}$$

This condition states that the cell cycle duration τ_S of the stem cells must be small enough for the solutions to be locally stable.

Only case 3 is of interest since it is the only one potentially leading to a loss of stability of the steady state and giving rise to oscillations. In the following analysis, case 3 will be assumed: $B_3 \leqslant -|B_2|$. When inequality (8) becomes an equality, a Hopf bifurcation occurs (Bernard et al., 2001) with period

$$T_{Hopf} = \frac{2\pi}{\sqrt{B_3^2 - B_2^2}}. \tag{9}$$

[5] Considerations of telomere loss during stems cell replication (Vickers et al., 2000) indicate that the differentiation rate F could be very small in humans compared to those in mice or dogs. This may explain why long period oscillations are sometimes observed in humans and not in grey collies. This also suggests that, in some cases, the source of oscillation in cyclical neutropenia may be different in human and grey collies (although the differences in parameter values between the two species may also account for a difference in the period).

When B_2 is negative, the arccos in inequality (8) is bounded below by $\pi/2$ and above by π. Thus, from Eqs. (8) and (9), it is easy to show that the period T_{Hopf} is restricted to the interval $[2\tau_S, 4\tau_S]$ for B_2 negative. In this case no long period oscillations can occur. However, if B_2 is positive and close to B_3, a Hopf bifurcation will have a Hopf period $T_{Hopf} \geqslant 4\tau_S$ and thus a long period bifurcation can occur if the denominator of Eq. (9) becomes small. We can even give an upper bound for the value T_{Hopf}. From the definition of B_2 and B_3 in Eq. (C.3), we have

$$B_3 < -2\exp(-\gamma_S\tau_S)B_2, \tag{10}$$

and as we are in case 3,

$$B_3^2 > 4\exp(-2\gamma_S\tau_S)B_2^2. \tag{11}$$

Inserting Eq. (11) into Eq. (9) leads to

$$T_{Hopf} < \frac{2\pi}{|B_2|\sqrt{4\exp(-2\gamma_S\tau_S)-1}}. \tag{12}$$

Refer to Fig. 2 to see what happens for each value of (B_2, B_3) in term of stability and bifurcation period. From Eq. (12) we see that it is necessary to have a large value of $\gamma_S\tau_S$ for a long Hopf period at the bifurcation point. Another requirement from Eq. (9) is that $B_3 \sim -B_2$, which can only happen when the differentiation rate F is small and $2\exp(-\gamma_S\tau_S)$ is near 1.

4.2. Numerical analysis of the model

The numerical analysis described in this section does not take the form of traditional numerical simulations since we used a `Matlab` package, `DDE-BIFTOOLS` (Engelborghs et al., 2001), which is based on continuation methods that are in widespread use for ordinary differential equations through the software `AUTO` (Doedel, 1981).

First assume that for a given value of A (large enough), the unique positive steady state is locally stable. When A is decreased, corresponding to an increased level of neutrophil precursor apoptosis, this steady state is destabilized (Mechanism 1). A second way to destabilize the system is by increasing the apoptosis rate γ_S in the HSC compartment (Mechanism 2). Figs. 3 and 4 show the bifurcation diagrams for the full model for changes

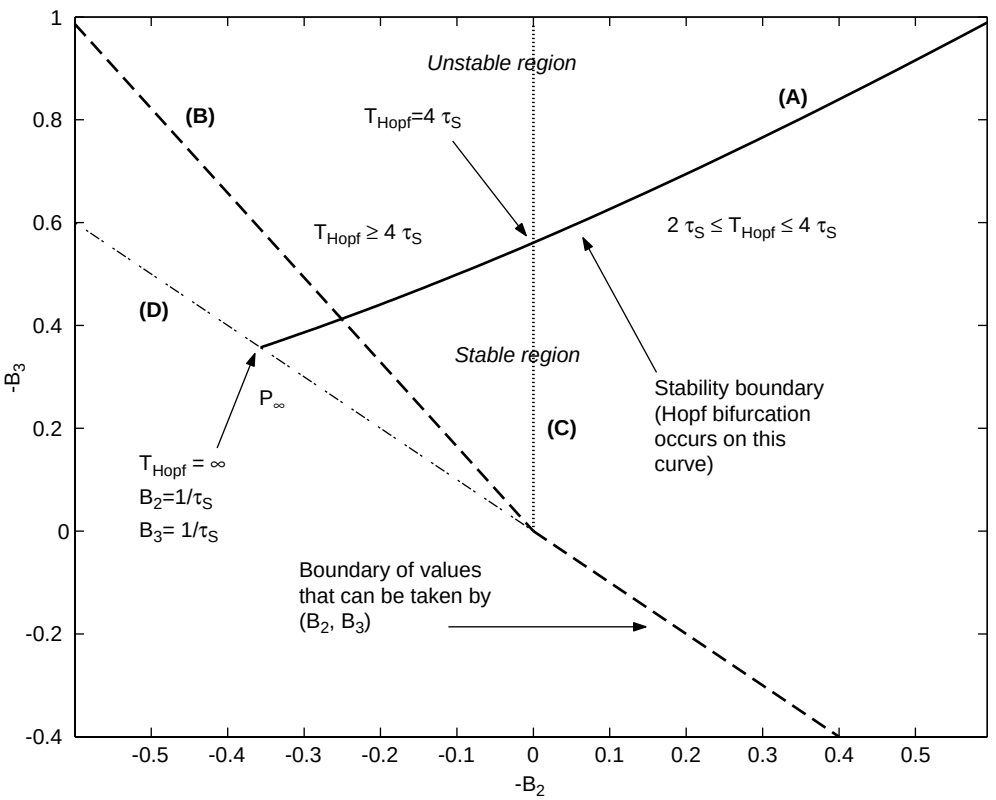

Fig. 2. Stability region in the B_2 B_3-plane when F is a constant. The stability region is below the thick curve (A) and to the right of the dashed line (B). The system becomes unstable through a Hopf bifurcation when (B_2, B_3) crosses the stability boundary (A). The period of oscillation at the bifurcation depends on the position of the bifurcation point relative to the dotted line (C). If the bifurcation occurs to the right of the dotted line, then $2\tau_S \leqslant T_{Hopf} < 4\tau_S$. If the bifurcation occurs to the left of the dotted line, then $T_{Hopf} \geqslant 4\tau_S$. The period increases when the bifurcation point goes to the left of the figure (B_2 more positive) and tends to infinity when the stability curve (A) meets the dashed–dotted curve (D) at point P_∞. The dashed curve (B) delimits the values that can be taken by (B_2, B_3). The upper part of line (B) has a slope of $2\exp-\gamma_S\tau_S > 1$ and approaches 1 when γ_S is increased. The only way for a bifurcation to occur near P_∞ is by either increasing τ_S or γ_S. The parameters used to plot this figure are $\gamma_S = 0.07\,\text{day}^{-1}$ and $\tau_S = 2.8$ days.

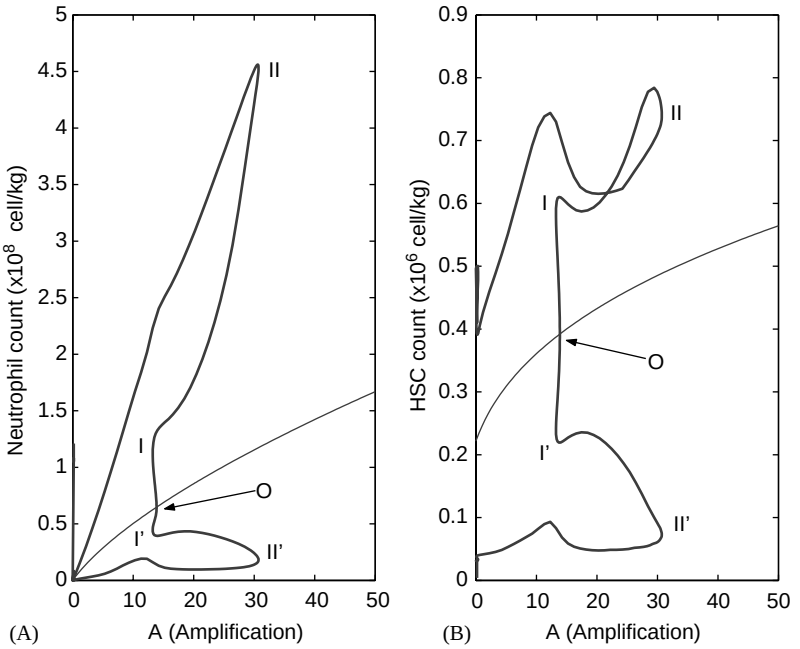

Fig. 3. Bifurcation diagrams for N (panel A) and S (panel B) with respect to the parameter A. In each panel, the thin line represents the steady state (N_*, S_*) and the thick lines represents the envelope of the periodic solution around that steady state (the envelope is defined by the maximum and the minimum oscillation values for each value of the parameter A). In both panels, the point O is a supercritical Hopf bifurcation, and when A is decreasing, the steady state is destabilized. At this point O ($A = 13.87$), a small stable limit cycle appears with increasing amplitude until its envelope reaches the points I and I′ (at $A = 13.24$). At this point the limit cycle disappears through a reverse saddle-node bifurcation of limit cycles (point I), together with an unstable limit cycle between points I and II ($A = 30.73$). This unstable limit cycle, with envelope defined by curves between points I and II and between I′ and II′, appears at a larger value of A (point II) through another saddle-node bifurcation of limit cycles together with a stable limit cycle of large amplitude. The large amplitude limit cycle exists from point II to $A = 0$, and coexists with a locally stable steady state up to point O, with a stable limit cycle between points O and I, and is the only attractor for A values to the left of point I. The steady state for N ranges from 0 to 1.7×10^8 cell/kg whereas S ranges from 0.22 to 0.56×10^6 cell/kg. Parameters used for this simulation as in Table 1.

in either the amplification A or the HSC apoptosis rate γ_S, respectively. From the numerical analysis, the destabilization of the fixed point in both cases occurs via a supercritical Hopf bifurcation (point O in Figs. 3 and 4). Before this bifurcation can be observed, the system undergoes a saddle-node bifurcation of limit cycles: a stable and an unstable limit cycle appear at points II in Figs. 3 and 4. This happens either when A decreases or when γ_S increases.

In Fig. 3, the bifurcation diagram is plotted for N_* and S_* with respect to A, and represents Mechanism 1. Four types of solutions can be found in the figure: stable steady-states, unstable steady-states, stable limit cycles and unstable limit cycles. The steady states (plotted in thin lines) range from 0 to 1.7×10^8 cell/kg for N_* and from 0.22 to 0.56×10^6 cell/kg for S_* when A goes from 0 to 50. These values of S_* are close to the normal steady state of 1.1×10^6 cell/kg, and can be explained by a robust adaptivity, a necessary condition for a system such as the hematopoietic system. Experimental data show that in neutropenic patients, the neutrophil count is around 0.12 of the normal value, whereas other cell lines do not show significant decreases in their level (Wright et al., 1981; Haurie et al., 1998). The relative independence of S_* with respect to A shows that the model presented here reproduces well this robustness of the HSC compartment and explains why other cell lineages show oscillations around their normal values in CN without depletion in their level.

However, the effect differs when we look at Fig. 4. Indeed, when γ_S is taken as the bifurcation parameter, the diagrams look similar to Fig. 3 qualitatively but things are different quantitatively. From a dynamical point of view, we can see that in both panels of Fig. 4, a supercritical Hopf bifurcation occurs at point O, and there is a small stable limit cycle as in the bifurcation diagram of A. The stable limit cycle disappears at point I through a saddle-node bifurcation of limit cycles and an unstable limit cycle joints points I and II. At point II, a large limit cycle appears and stays until $\gamma_S = 0.20\,\text{day}^{-1}$, after which the numerical continuation method failed to follow the periodic solution. If we look at the steady states, we note that N_* goes from 0.45 to 1.0×10^8 cell/kg and S_* from 0.14 to 0.58×10^6 cell/kg when the HSC apoptosis rate γ_S goes from 0 to $0.20\,\text{day}^{-1}$. The situation is reversed from the bifurcation diagram with A. Now the HSC steady-state level S_* is decreased by a factor 4 while the neutrophil count decreases by a factor 2. The HSC apoptotic rate γ_S is a sensitive parameter, and small changes can have deleterious effects in the

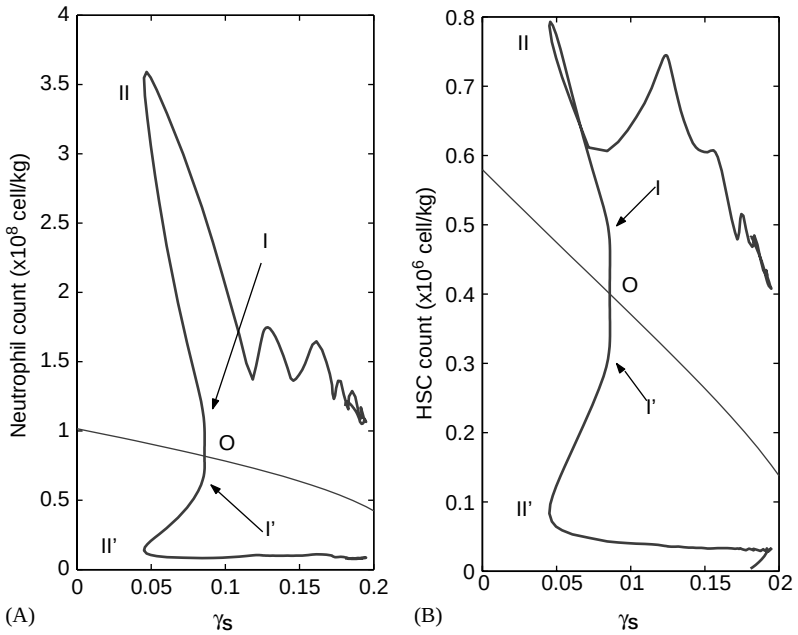

Fig. 4. Bifurcation diagrams for N (panel A) and S (panel B) with respect to parameter γ_S. In each panel, the thin line represents the steady state (N_*, S_*) and the thick line represents the envelope of the periodic solution around that steady state. In both panels, the point O corresponds to a supercritical Hopf bifurcation, and when γ_S is increasing, the steady state is destabilized. At this point O ($\gamma_S = 0.08589\,\text{day}^{-1}$), a small stable limit cycle appears with increasing amplitude until its envelope reaches the point I and I′ (at $\gamma_S = 0.08606\,\text{day}^{-1}$). At this point the limit cycle disappears through a reverse saddle-node bifurcation of limit cycles (point I), together with an unstable limit cycle between points I and II ($\gamma_S = 0.045\,\text{day}^{-1}$). This unstable limit cycle, with envelope defined by curves between points I and II and between I′ and II′, appears at a larger value of A (point II) through another saddle-node bifurcation of limit cycles together with a stable limit cycle of large amplitude. The large amplitude limit cycle exists from point II to γ_S near 0.20, and coexists with a locally stable steady state up to point O, with a stable limit cycle between points O and I, and is the only attractor for γ_S values to the right of point I. What happens when γ_S approaches is not clear numerically. Note the scale for each panel, the steady state for N ranges from 0.45 to 1.0×10^8 cell/kg whereas S ranges from 0.14 to 0.58×10^6 cell/kg. Parameters used are as in Table 1 except $A = 20$.

HSC level. In fact, if the apoptotic rate is high enough, less than one daughter cell will come out of the proliferative phase for each mother cell entering the cell cycle. If

$$\gamma_S > \frac{\ln 2}{\tau_S}, \tag{13}$$

then the HSC count will decrease to zero, meaning that the hematopoietic system can no longer produce blood cells (note that condition (5) holds this case). This situation is never encountered when A is changed; even when $A = 0$ the steady state $S_* > 0$. For that reason, we hypothesize that the most important source for the onset of oscillations in CN is an elevated apoptotic rate in the recognizable and committed neutrophil precursors (Mechanism 1).

Another piece of evidence supporting the hypothesis that CN in grey collies is due to a higher than normal apoptosis rate in the neutrophil precursors is given by looking at the period of oscillation with respect to A and γ_S in Fig. 5. In panel (A) the period is plotted as a function of A. For values of A between 12 and 30, the period of the stable limit cycle is almost constant, ranging from 14 to 16 days. These values corresponds to the ones seen in grey collies with CN. This range from 12 to 30 is also an acceptable range for A when the model is fitted to experimental data. The rapidly falling period as A becomes smaller than 15 occurs at the same time than the disappearance of the stable limit cycle (point I in Figs. 3 and 5, panels (A)).

In Fig. 5(B), the period of oscillation is plotted as a function of γ_S. As we can see, for a short range ($\gamma_S = 0.05-0.12\,\text{day}^{-1}$), the period is almost constant around 16–17 days. For larger apoptosis rates, the period increases rapidly and reaches nearly 30 days when $\gamma_S = 0.20\,\text{day}^{-1}$. These long period oscillations have been observed in humans with CN (Haurie et al., 1998), and an increase in HSC apoptosis could, in some cases, play a role.

5. Model simulations of neutrophil oscillation

5.1. Periodic solutions behaviour

We performed numerical simulations on the full model (1,2) using the software `xppaut` (Ermentrout, 2001, 2002).

Fig. 6 shows two types of periodic solutions that can exist in CN. In panel (A) is shown a small amplitude

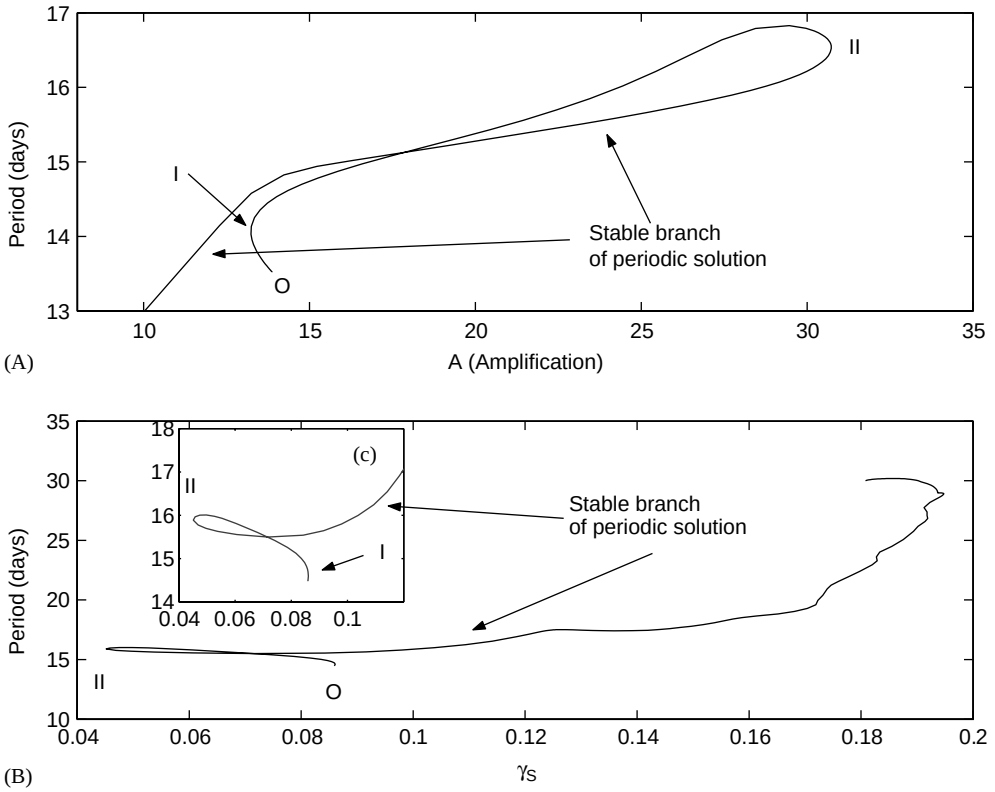

Fig. 5. Period of oscillation of the system with respect to bifurcation parameters A (panel A) and S (panel B). In each panel, the period of each existing limit cycle is plotted. The numbering O, I and II refers to Figs. 3 and 4 where the corresponding points are shown. In panel (A), the period of oscillation shows a plateau for the stable branch for values of A between 12 and 30. In panel (B), a large increase is seen when S approaches $0.20\,\text{day}^{-1}$. In panel (C) is a enlargement of the left part of the curve to show details of the intersection and turning points I and II.

periodic solution, which had appeared through the Hopf bifurcation (point O in Fig. 3). This periodic solution does not exist for a large window of A values, thus it is not likely to be experimentally observable. However, in Fig. 6(B), the periodic solution, which appeared through the saddle-node bifurcation, is representative of the behaviour of neutrophil counts in grey collies. The neutrophil count goes from nearly zero to a normal level with a characteristic secondary bump on the falling phases. This second mode in the neutrophil oscillation in grey collies has been shown to be due to the interaction of the delay τ_N and the periodic input of HSC into the neutrophil lineage (Bernard et al., 2001).

5.2. Effect of G-CSF administration

In Fig. 7 we have simulated the effect of administrating G-CSF to a neutropenic dog. Five effects of G-CSF were considered:

- decrease of apoptosis in neutrophil precursors, leading to an increase in A,
- increase in the HSC differentiation rate F, by increasing θ_1. The parameter θ_1 is proportional to the production of G-CSF;
- decrease of apoptosis γ_S of HSC;
- decrease of the proliferative phase duration τ_S of HSC; and
- decrease of the neutrophil precursors transit time τ_N

Clinical studies have shown that administrating G-CSF to patients with CN usually results in a net increase of the mean neutrophil count, in the amplitude of oscillation and in the minimum neutrophil count, and a decrease in the period of oscillation (Hammond et al., 1989). The same effects have been observed in grey collies following G-CSF treatment (Haurie et al., 2000). Fig. 7 shows all of these changes when G-CSF administration is simulated with the above-mentioned changes in the model parameters.

6. A new hypothesis for the origin of oscillations in cyclical neutropenia

The results of Sections 4.1 and 4.2 suggest a new hypothesis concerning the onset of oscillations seen in CN. Namely:

We hypothesize that the cause of the oscillations in CN is a destabilization in the hematopoietic stem cell

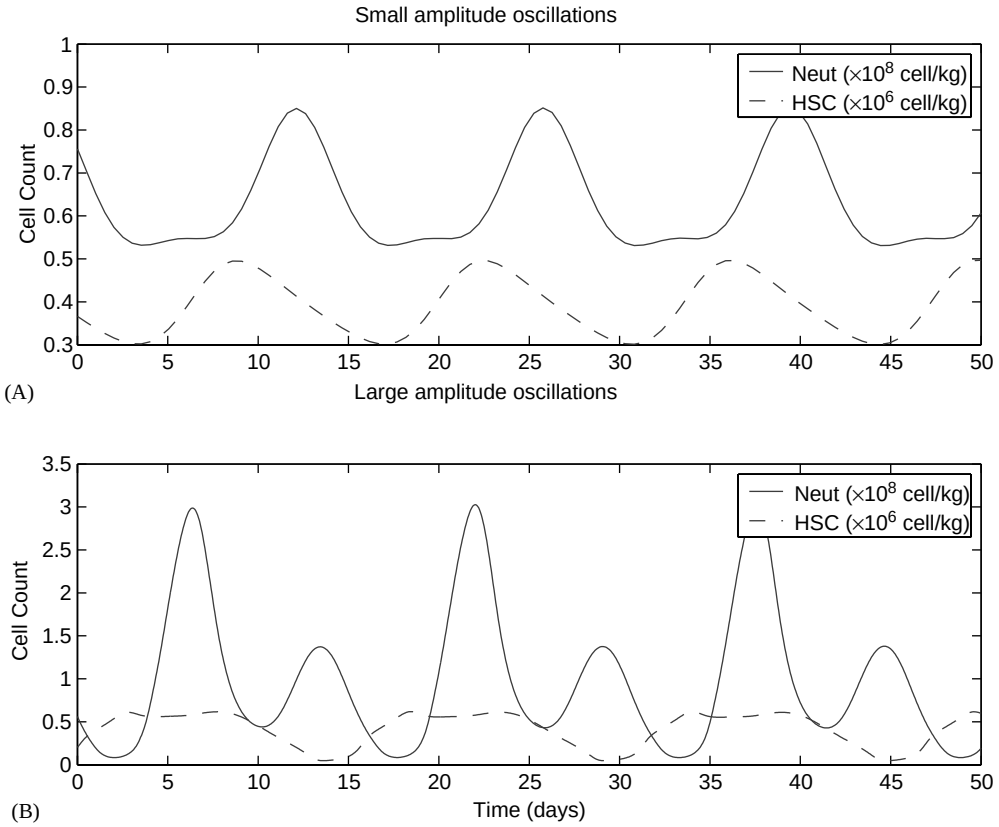

Fig. 6. Small and large oscillations in the neutrophil and HSC count. Parameters as in Table 1 except $A = 13.50$ in panel (A) and $A = 20.0$ in panel (B).

regulatory system due to an elevated apoptotic rate in the recognizable and committed neutrophil precursors.

This elevation has been observed experimentally (Aprikyan et al., 2001) but a link between elevated apoptosis in committed neutrophil precursors and oscillations in the stem cell compartment has not been clear until now.

Oscillations seen in other cell lineages—reticulocytes, monocytes, platelets, lymphocytes—(Haurie et al., 1999a) further support the idea that the origin of this disorder lies in the primitive bone marrow cell population. In Fig. 3, the mean HSC level is about 50% normal, whereas the neutrophil level undergoes a ten-fold decrease from normal values in CN. This small decrease in HSC level compared to the neutrophil level explains why the mean level of other blood cell lines are relatively unaffected by CN. The regulation mechanisms in these lines are robust enough to compensate for a periodic decrease in HSC level (this is confirmed by numerical simulations, not shown here). We propose this oscillation mechanism as a generic way to introduce oscillations in hematopoiesis. It could, for instance, explain oscillations of period between 16 and 19 days seen in erythrocyte levels after marrow irradiation in mice (Gurney et al., 1981; Gibson et al., 1984, 1985).

7. Discussion

CN is a rare disorder characterized by oscillatory production of blood cells in the bone marrow. The oscillations are most prominent in the neutrophil count, but are also present in other cell lineages (lymphocytes, reticulocytes, monocytes and platelets). In this study, we have developed a physiologically realistic mathematical model for neutrophil production from the HSC. We tested the hypothesis that the oscillations of CN originate from the HSC (Haurie et al., 2000; Hearn et al., 1998) as a secondary response to a primary increased rate of apoptosis (mimicked by a decrease in the value of the parameter A) in the recognizable neutrophil precursors (Aprikyan et al., 2001). Our numerical simulations show that increasing the apoptosis rate in the neutrophil regulatory system leads to an increased demand on the HSC with a consequent destabilization of the steady-state number of stem cells and the appearance of oscillations through a Hopf bifurcation

Discrepancies between experimental data or indirect measurements of parameters make the parameter estimation procedure difficult. One of the most difficult parameters to estimate is the HSC level in normal dogs. Abkowitz et al. (2002) hypothesized that the absolute

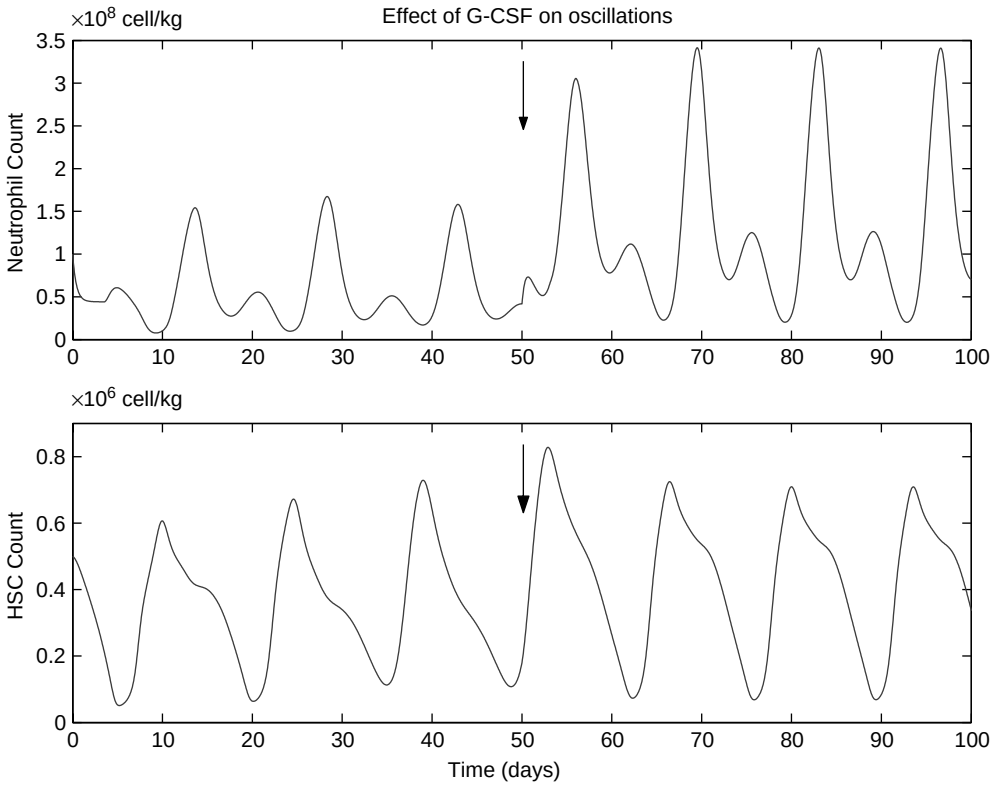

Fig. 7. Effect of G-CSF administration on the circulating neutrophil and HSC counts. Beginning on day 50 (vertical arrow), continuous G-CSF administration was simulated by changing five parameters in the following way: A from 10–20, θ_1 from 0.36 to 0.80×10^8 cell/kg, γ_S from 0.07 to $0.05\,\text{day}^{-1}$, τ_S from 2.8 to 2.6 days and τ_N from 3.5 to 3.0 days.

number of HSC is approximately constant among all mammals. Implications of this claim are numerous, one of them being that in larger mammals, like dogs or humans, the hematopoietic system must work differently than in small mammals in order to meet their blood cell production requirements. As many parameters depend on S_*, a judicious choice must be made.

Another problem raised by stem cell kinetic parameter estimation is translating to humans the model presented here, as few kinetic data for human stem cells in vivo are available. To obtain a better understanding of the dynamical features of hematological disorders, kinetic data for humans have to be determined. Existing technologies, such as cell markers, could help to attain this goal. These kinetic data would be of great potential to help in designing more efficient protocols for bone marrow transplants.

Despite the parameter estimation problems, the model presented here captures the essentials of the white blood cell regulatory system in CN. Both experimental data and numerical simulations indicate that regulated apoptosis may be a powerful control mechanism for the production of blood cells and that the loss of control over apoptosis can have significant and negative effects on the dynamical properties of hematopoiesis. Thus, with a decrease in apoptotic rate the hematopoietic system can respond rapidly to an increased demand for circulating blood cells. To make this comment clearer, as pointed out by the normal input to the post-mitotic neutrophil compartment is about 2.3 times the GTR and thus a reduction of the rate of apoptosis to zero would more than double the GTR. This means, for example, that a substantial fall in neutrophil numbers would lead to an increased level of circulating G-CSF. This would, in turn, lead to a decreased level of apoptosis and consequent increase in the GTR. This elevated effective production of neutrophils would also be felt rapidly since the increased levels of G-CSF would not only decrease the level of apoptosis but also decrease the time spent in the post-mitotic compartment as has been documented by Chatta et al. (1994) and Price et al. (1996).

Analytical examination of the model also showed that an increase in the rate of stem cell apoptosis can lead to long period oscillations in the neutrophil count. This could be a factor in the difference between periods observed in dogs and in humans (14 vs. 21 days). However, there is no evidence at this time that the rate of stem cell apoptosis is higher than normal in CN.

The clinical effects of G-CSF administration have been successfully simulated by varying parameters

known to be affected by G-CSF. The amplitude, mean level and nadir of the oscillation increased, while the period decreased following G-CSF administration.

Our results are thus consistent with the hypothesis that CN originates from an elevation of apoptosis rates in the peripheral neutrophil regulatory system that destabilizes the HSC dynamics leading to the oscillatory pattern observed clinically.

Another hematological disease in which oscillations in leukocytes, platelets and erythrocyte precursors can be seen is periodic chronic myelogenous leukemia (PCML) (Fortin and Mackey, 1999). This form of leukemia is characterized by oscillations from normal to high levels in leukocyte count with periods ranging from 35 to 80 days. A relationship exists between some kinds of neutropenia and leukemia since it has been established that some neutropenic patients will eventually develop leukemia (Lensink et al., 1986; Weinblatt et al., 1995; Freedman et al., 2000; Jeha et al., 2000; Dinauer et al., 2000). An interesting question which we are now exploring is whether there exists a causal link between CN and PCML in terms of the dynamics of hematopoietic regulation.

Acknowledgements

We thank Prof. David Dale and Ms. Caroline Haurie for the grey collie data and an anonymous referee for detailed suggestions. This work was supported by MITACS (Canada), the Natural Sciences and Engineering Research Council (NSERC Grant OGP-0036920, Canada), the Alexander von Humboldt Stiftung, Le Fonds pour la Formation de Chercheurs et l'Aide à la Recherche (FCAR grant 98ER1057, Québec), the Leverhulme Trust (UK) and the Institut des Sciences mathématiques (ISM, Québec).

Appendix A. Formulation of the feedback functions F and K

Recent studies show that a significant degree of G-CSF clearance is performed by the binding of G-CSF by G-CSF receptors located on the surface of neutrophils (Layton et al., 1989; Kato et al., 1997; Stefanich et al., 1997). This binding allows the activation of mechanisms leading to enhanced cell survival (Williams et al., 1990; Borge et al., 1997), increased proliferation and an increased differentiation rate (Haurie et al., 1998; Kanayasu-Toyoda et al., 1999). Even if the exact activation pathway is poorly understood, one can assume that the cellular response is proportional to the number of activated (bound) G-CSF receptors per cell. Assuming that G-CSF binds to the receptor following the law of mass action, we can determine the dependence of the differentiation rate on G-CSF.

Let $[G]$ denote the G-CSF concentration, $[R]$ the density of free receptors, $[L]$ the density of activated receptors and $[N]$ the concentration of neutrophils and their precursors. The total number of receptors is

$$[R] + [L] = m[N], \tag{A.1}$$

where m is average number of G-CSF receptors per cell. R can represent dimer or oligomer receptors. If n G-CSF molecules are required to activate one receptor, then from the law of mass action

$$[R] + n[G] \rightleftharpoons [L]. \tag{A.2}$$

At equilibrium we have

$$[R][G]^n = k[L], \tag{A.3}$$

where k is a reaction coefficient. We assume that the differentiation rate F is proportional to the fraction of bound receptors on a cell

$$F = f_0 \frac{[L]}{mN}. \tag{A.4}$$

From Eqs. (A.1) and (A.3) we obtain

$$[L] = \frac{m[N][G]^n}{k + [G]^n}. \tag{A.5}$$

Using Eq. (A.4), and dropping the brackets, we arrive at

$$F(G) = f_0 \frac{G^n}{k + G^n}. \tag{A.6}$$

G is mainly regulated by the number N of neutrophils such that the clearance of G by N is linear with proportionality constant σ (Terashi et al., 1999; Takatani et al., 1996) and the production P is constant. Thus, the concentration of G-CSF is represented by the equation

$$\dot{G} = P - \sigma NG. \tag{A.7}$$

The G-CSF clearance becomes saturated when the level of G-CSF increases (Hayashi et al., 2001), but in this study we assume that this effect is unimportant. This will keep the formulation in the following as simple as possible. Then the steady state is

$$G_* = \frac{P}{\sigma N}. \tag{A.8}$$

Replacing G in Eq. (A.6) by its steady-state value G_* gives

$$\begin{aligned} F(G) &= F(G(N)) = \tilde{F}(N) \\ &= f_0 \frac{(P/\sigma N)^n}{(P/\sigma N)^n} = f_0 \frac{\tilde{k}}{\tilde{k} + N^n}, \end{aligned} \tag{A.9}$$

where

$$\tilde{k} = \frac{P^n}{k\sigma^n}. \tag{A.10}$$

From these considerations, we take F to be of the form

$$F(N) = f_0 \frac{\theta_1^n}{\theta_1^n + N^n} \tag{A.11}$$

with $\theta_1^n = \tilde{k}$. Notice that θ_1 depends on the production of G-CSF; this parameter will be affected by administration of exogenous G-CSF. Function F is a Hill function and the exponent n is often referred as a Hill coefficient or a cooperativity coefficient. We can perform much the same derivation for the feedback function K to obtain the same form as in Mackey et al. (2003) and Andersen and Mackey (2001):

$$K(S) = k_0 \frac{\theta_2^s}{\theta_2^s + S^s}. \tag{A.12}$$

Appendix B. Existence and uniqueness of the steady state

We present here the details of computations carried out in Section 4. In this section we present the proof of the existence and uniqueness of the positive steady state under condition (5). First write the equations for the steady states

$$\alpha N_* = AF(N_*)S_* \tag{B.1}$$

and

$$F(N_*) = rK(S_*), \tag{B.2}$$

where $r = 2\exp(-\gamma_S\tau_S) - 1$. From the definition of $K(S)$, Eq. (A.12), and Eq. (B.2) we can find the steady state S_* in term of N_*,

$$S_* = \theta_2 \sqrt{\left(\frac{rk_0}{F(N_*)} - 1\right)}. \tag{B.3}$$

From Eq. (B.1) and (B.3), we can eliminate S_*,

$$N_* = \frac{A\theta_2}{\alpha} \sqrt{\left(\frac{rk_0}{F(N_*)} - 1\right)} F(N_*). \tag{B.4}$$

Let the right-hand side of Eq. (B.4) be $G(N_*)$. Then the derivative of G with respect to N_* is,

$$G'(N_*) = \frac{A\theta_2}{2\alpha} \sqrt{\left(\frac{rk_0}{F(N_*)} - 1\right)} F'(N_*) \times \left[2 - \frac{2}{1 - F(N_*)(rk_0)^{-1}}\right]. \tag{B.5}$$

If we can prove that $G'(N_*)$ is always negative, then by using the fixed point theorem it is easy to show that there exists one and only one positive steady state N_*, and from that value the uniqueness of the steady state S_* follows naturally. To show that $G'(N^*)$ is negative, we have only to make sure that the factor in the brackets in Eq. (B.5) is positive since the rest is negative (from the definition of $F(N)$ in Eq. (A.11), it is obvious that $F_1(N) < 0$). So, we need to find conditions for which

$$2 - \frac{1}{1 - F(N_*)(rk_0)^{-1}} > 0. \tag{B.6}$$

This is equivalent to showing that

$$F(N_*) < \tfrac{1}{2} rk_0. \tag{B.7}$$

We know that $F(N_*) < f_0$, so a sufficient condition for $G'(N_*)$ to be negative is

$$f_0 < \tfrac{1}{2} rk_0 = \tfrac{1}{2}(2\exp(-\gamma_S\tau) - 1)k_0, \tag{B.8}$$

which completes the proof of the existence and uniqueness of the steady state (N_*, S_*) under condition (5).

Appendix C. Linearization and characteristic equation

The linearization of Eqs. (1) and (2) around the unique positive steady state (N_*, S_*) is performed as follow. First define new variables $x = N - N_*$ and $y = S - S_*$ so that $x = 0$ and $y = 0$ are fixed points. Then by linearizing around the steady state (N_*, S_*), we obtain

$$\frac{dx}{dt} = A_1 x + A_2 x_{\tau_N} + A_3 y_{\tau_N}, \tag{C.1}$$

and

$$\frac{dy}{dt} = B_1 x + B_2 y + B_3 y_{\tau_S}, \tag{C.2}$$

where the linearization coefficients are:

$$\begin{aligned} A_1 &= -\alpha = (-\alpha N)_N, \\ A_1 &= AF'_* S_* = (AF(N)S)_N, \\ A_3 &= AF_* = (AF(N)S)_S, \\ B_1 &= -F'_* S_* = (-F(N)S)_N, \\ B_2 &= -[F_* + K'_* S_* + K_*] = (-[F(N) + K(S)]S)_S, \\ B_3 &= 2\exp(-\gamma_S\tau_S)(K'_* S_* + K_*) \\ &= 2\exp(-\gamma_S\tau_S)(K(S)S)_S. \end{aligned} \tag{C.3}$$

The subscripts in the right-hand side equalities denote the partial derivative with respect to the variable. The star subscript $(*)$ in the middle equality means that the function is evaluated at the steady state and the prime stands for the derivative with respect to the argument. These equations can be formulated in a vector equation

$$\frac{dX}{dt} = LX + R_N X_{\tau N} + R_S X_{\tau S}, \tag{C.4}$$

where

$$X = \begin{pmatrix} x \\ y \end{pmatrix} \tag{C.5}$$

and

$$L = \begin{pmatrix} A_1 & 0 \\ B_1 & B_2 \end{pmatrix}, \quad R_N = \begin{pmatrix} A_2 & A_3 \\ 0 & 0 \end{pmatrix},$$
$$R_S = \begin{pmatrix} 0 & 0 \\ 0 & B_3 \end{pmatrix}. \tag{C.6}$$

The characteristic equation of Eq. (C.4) is defined as

$$\det[\lambda I - L - R_N \exp(-\lambda_{\tau N}) - R_S \exp(\lambda_{\tau S})] = 0 \tag{C.7}$$

with I the 2×2 identity matrix. The characteristic equation can then be explicitly written as Eq. (6).

References

Abkowitz, J.L., Catlin, S.N., McCallie, M.T., Guttorp, P., 2002. Evidence that the number of hematopoietic stem cells per animal is conserved in mammals. Blood 100, 2665–2667.

Abkowitz, J.L., Golinelli, D., Harrison, D.E., Guttorp, P., 2000. In vivo kinetics of murine hemopoietic stem cells. Blood 96, 3399–3405.

Akbarzadeh, S., Ward, A.C., McPhee, D.O.M., Alexander, W.S., Lieschke, G.J., Layton, J.E., 2002. Tyrosine residues of the granulocyte colony-stimulating factor receptor transmit proliferation and differentiation signals in murine bone marrow cells. Blood 99, 879–887.

Andersen, L.K., Mackey, M.C., 2001. Resonance in periodic chemotheray: a case study of acute myelogenous leukemia. J. Theor. Biol. 209, 113–130.

Aprikyan, A.A.G., Liles, W.C., Rodger, E., Jonas, M., Chi, E.Y., Dale, D.C., 2001. Impaired survival of bone marrow hematopoietic progenitor cells in cyclic neutropenia. Blood 97, 147–153.

Bagley, C.J., Woodcock, J.M., Stomski, F.C., Lopez, A.F., 1997. The structural and functional basis of cytokine receptor activation: lessons from the common subunit of the granulocyte-macrophage colony-stimulating factor, interleukin-3 (IL-3), and IL-5 receptors. Blood 89, 1471–1482.

Basu, S., Hodgson, G., Katz, M., Dunn, A.R., 2002. Evaluation of role of G-CSF in the production, survival, and release of neutrophils from bone marrow into circulation. Blood 100, 854–861.

Bernard, S., Bélair, J., Mackey, M.C., 2001. Sufficient conditions for stability of linear differential equations with distributed delays. Discrete Contin. Dyn. System Ser. B 1, 233–256.

Bernard, S., Pujo-Menjouet, L., Mackey, M.C., in review. Analysis of cell kinetics using a cell division marker: mathematical modeling of experimental data, in review.

Boggs, D., Boggs, S., Saxe, D., Gress, L., Canfield, D., 1982. Hematopoietic stem cells with high proliferative potential assay of their concentration in marrow by the frequency and duration of cure of W/Wv mice. J. Clin. Invest. 70, 242–253.

Borge, O.J., Ramsfjell, V., Cui, L., Jacobsen, S.E., 1997. Ability of early acting cytokines to directly promote survival and suppress apoptosis of human primitive CD34+CD38-bone marrow cells with multilineage potential at the single cell level: key role of thrombopoietin. Blood 90, 2282–2292.

Bradford, G., Williams, B., Rossi, R., Bertoncello, I., 1997. Quiescence, cycling, and turnover in the primitive hematopoietic stem cell compartment. Exp. Hematol. 25, 445–453.

Burthem, J., Mottram, R., Lucas, G.S., Whetton, A.D., unpublished. Imatinib mesilate (STI571) causes an increased rate of maturation and a reduced expansion of cell number during the granulocytic differentiation of CD34+cells from CML patients, unpublished.

Chatta, G., Price, T., Allen, R., Dale, D., 1994. Effects of in vivo recombinant methionyl human granulocyte colony stimulating factor on the neutrophil response and peripheral blood colony forming cells in healthy young and elderly adult volunteers. Blood 84, 2923–2929.

Cheshier, S., Morrison, S., Liao, X., Weissman, I., 1999. In vivo proliferation and cell cycle kinetics of long term self renewing haematopoietic stem cells. Proc. Natl Acad. Sci. USA 96, 3120–3125.

Dale, D.C., Hammond, W.P., 1988. Cyclic neutropenia: a clinical review. Blood Rev. 2, 178–185.

Dale, D.C., Person, R.E., Bolyard, A.A., Aprikyan, A.G., Bos, C., Bonilla, M.A., Boxer, L.A., Kannourakis, G., Zeidler, C., Welte, K., Benson, K.F., Horwitz, M., 2000. Mutations in the gene encoding neutrophil elastase in congenital and cyclic neutropenia. Blood 96, 2317–2322.

Deubelbeiss, K.A., Dancey, J.T., Harker, L.A., Finch, C.A., 1975. Neutrophil kinetics in the dog. J. Clin. Invest. 55, 833–839.

Dinauer, M.C., Lekstrom-Himes, J.A., Dale, D.C., 2000. Inherited Neutrophil disorders: molecular basis and new therapies. Hematology 2000, 303–318.

Doedel, E.J., 1981. Auto: A program for the automatic bifurcation analysis of autonomous systems. In: Proceedings of the 10th Manitoba Conference on Numerical Mathematics and Computations, University of Manitoba, Winnipeg, Canada, pp. 265–284.

Edelstein-Keshet, L., Israel, A., Lansdorp, P., 2001. Modelling perspective on aging: can mathematics help us stay young? J. Theor. Biol. 213, 509–525.

Engelborghs, K., Luzyanina, T., Samaey, G., 2001. DDE-BIFTOOL v. 2.00: a matlab package for bifurcation analysis of delay differential equations, Katholieke Universiteit Leuven, http://www.cs.kuleuven.ac.be/koen/

Ermentrout, B., 2001. XPPAUT version 5.4 software, http://www.math.pitt.edu/bard/xpp/xpp.html

Ermentrout, B., 2002. Simulating, Analyzing, and Animating Dynamical Systems: A Guide to Xppaut for Researchers and Students (Software, Environments, Tools), 1st Edition. SIAM, Philadelphia, PA.

Fortin, P., Mackey, M.C., 1999. Periodic chronic myelogenous leukemia: spectral analysis of blood cell counts and aetiological implications. Br. J. Haematol. 104, 336–345.

Fowler, A.C., Mackey, M.C., 2002. Relaxation oscillations in a class of delay differential equations. SIAM J. Appl. Math. 63, 299–327.

Freedman, M.H., Bonilla, M.A., Fier, C., Bolyard, A.A., Scar-lata, D., Boxer, L.A., Brown, S., Cham, B., Kannourakis, G., Kinsey, S.E., Mori, P.G., Cottle, T., Welte, K., Dale, D.C., 2000. Myelodysplasia syndrome and acute myeloid leukemia in patients with congenital neutropenia receiving G-CSF therapy. Blood 96, 429–436.

Gibson, C., Gurney, C., Gaston, E., Simmons, E., 1984. Cyclic erythropoiesis in the S_1/S_1^d mouse. Exp. Hematol. 12, 343–348.

Gibson, C., Gurney, C., Simmons, E., Gaston, E., 1985. Further studies on cyclic erythropoiesis in mice. Exp. Hematol. 13, 855–860.

Guerry, D.H., Dale, D.C., Omine, M., Perry, S., Wolff, S.M., 1973. Periodic hematopoiesis in human cyclic neutropenia. J. Clin. Invest. 52, 3220–3230.

Gurney, C., Simmons, E., Gaston, E., 1981. Cyclic erythropoiesis in W/W^v mice following a single small dose of ^{89}SR. Exp. Hematol. 9, 118–122.

Hammond, W.P., Price, T.H., Souza, L.M., Dale, D.C., 1989. Treatment of cyclic neutropenia with granulocyte colony stimulating factor. N. Eng. J. Med. 320, 1306–1311.

Harrison, D., Astle, C., Lerner, C., 1988. Number and continuous proliferative pattern of transplanted primitive immunohematopoietic stem cells. Proc. Natl Acad. Sci. USA 85, 822–826.

Haurie, C., Dale, D.C., Mackey, M.C., 1998. Cyclical neutropenia and other periodic hematological diseases: a review of mechanisms and mathematical models. Blood 92, 2629–2640.

Haurie, C., Dale, D.C., Mackey, M.C., 1999a. Occurrence of periodic oscillations in the differential blood counts of congenital, idiopathic and cyclical neutropenic patients before and during treatment with G-CSF. Exp. Hematol. 27, 401–409.

Haurie, C., Person, R., Dale, D.C., Mackey, M.C., 1999b. Haematopoietic dynamics in grey collies. Exp. Hematol. 27, 1139–1148.

Haurie, C., Dale, D.C., Rudnicki, R., Mackey, M.C., 2000. Modeling complex neutrophil dynamics in the grey collie. J. Theor. Biol. 204, 505–519.

Hayashi, N., Aso, H., Higashida, M., Kinoshita, H., Ohdo, S., Yukawa, E., Higuchi, S., 2001. Estimation of RHG-CSF absorption kinetics after subcutaneous administration using a modified Wagner–Nelson method with a nonlinear elimination model. Eur. J. Pharm. Sci. 13, 151–158.

Hayes, N., 1950. Roots of the transcendental equation associated with a certain difference-differential equation. J. London Math. Soc. 25, 226–232.

Hearn, T., Haurie, C., Mackey, M.C., 1998. Cyclical neutropenia and the peripheral control of white blood cell production. J. Theor. Biol. 192, 167–181.

Jeha, S., Chan, K.W., Aprikyan, A.G., Hoots, W.K., Culbert, S., Zietz, H., Dale, D.C., Albitar, M., 2000. Spontaneous remission of granulocyte colony-stimulating factor-associated leukemia in a child with severe congenital neutropenia. Blood 96, 3647–3649.

Kanayasu-Toyoda, T., Yamaguchi, T., Uchida, E., Hayakawa, T., 1999. Commitment of neutrophilic differentiation and proliferation of HL-60 cells coincides with expression of transferrin receptor. Effect of granulocyte colony stimulating factor on differentiation and proliferation. J. Biol. Chem. 274, 25471–25480.

Kato, M., Kamiyama, H., Okazaki, A., Kumaki, K., Kato, Y., Sugiyama, Y., 1997. Mechanism for the nonlinear pharmacokinetics of erythropoietin in rats. Rats J. Pharmacol. Exp. Ther. 283, pp. 520–527.

Kazarinoff, N.D., van den Driessche, P., 1979. Control of oscillations in hematopoiesis. Science 203, 1348–1350.

Kearns, C.M., Wang, W.C., Stute, N., Ihle, J.N., Evans, W.E., 1993. Disposition of recombinant human granulocyte colony stimulating factor in children with severe chronic neutropenia. J. Pediatr. 123, 471–479.

King-Smith, E.A., Morley, A., 1970. Computer simulation of granulopoiesis: Normal and impaired granulopoiesis. Blood 36, 254–262.

Layton, J.E., Hockman, H., Sheridan, W.P., Morstyn, G., 1989. Evidence for a novel in vivo control mechanism of granulopoiesis: mature cell-related control of a regulatory growth factor. Blood 74, 1303–1307.

Lebowitz, J.L., Rubinow, S.I., 1969. Grain count distributions in labeled cell populations. J. Theor. Biol. 23, 99–123.

Lensink, D.B., Barton, A.B., Appelbaum, R.R., Hammond, W.P., 1986. Cyclic neutropenia as a premalignant manifestation of acute lymphoblastic leukemia. Am. J. Hematol. 22, 9–16.

Lotem, J., Sachs, L., 1988. In vivo control of differentiation of myeloid leukemic cells by recombinant granulocyte-macrophage colony-stimulating factor and interleukin 3. Blood 71, 375–382.

Lund, J.E., Padgett, G.A., Ott, R.L., 1967. Cyclic neutropenia in grey collie dogs. Blood 29, 452–461.

Lyons, A.B., 1999. Divided we stand: tracking cell proliferation with carboxy uorescein diacetate succinimidyl ester. Immunol. Cell Biol. 77, 509–515.

MacDonald, N., 1978. Cyclical neutropenia: models with two cell types and two time lags. In: Valleron, A., Macdonald, P. (Eds.), Biomathematics and Cell Kinetics. Elsevier/North-Holland, Amsterdam, pp. 287–295.

Mackey, M.C., 1978. A unified hypothesis for the origin of aplastic anemia and periodic haematopoiesis. Blood 51, 941–956.

Mackey, M.C., 2001. Cell kinetic status of hematopoietic stem cells. Cell Prolif. 34, 71–83.

Mackey, M.C., Aprikyan, A.A.G., Dale, D.C., 2003. The rate of apotosis in post mitotic precursors of normal and neutropenic human. Cell Prolif. 36, 27–34.

Mahaffy, J.M., Bélair, J., Mackey, M.C., 1998. Hematopoietic model with moving boundary condition and state dependent delay: applications in erythropiesis. J. Theor. Biol. 190, 135–146.

McCarthy, K.F., 1997. Population size and radiosensitivity of murine hematopoietic endogenous long-term repopulating cells. Blood 89, 834–841.

Mckinstry, W.J., Li, C.L., Rasko, J.E., Nicola, N.A., Johnson, G.R., Metcalf, D., 1997. Cytokine receptor expression on hematopoietic stem and progenitor cells. Blood 89, 65–71.

Micklem, H., Lennon, J., Ansell, J., Gray, R.A., 1987. Numbers and dispersion of repopulating hematopoietic cell clones in radiation chimeras as functions of injected cell dose. Exp. Hematol. 15, 251–257.

Morley, A., 1970. Periodic diseases, physiological rhythms and feedback control–a hypothesis. Aust. Ann. Med. 3, 244–249.

Morley, A., King-Smith, E.A., Stohlman, F., 1969. The oscillatory nature of hemopoiesis. In: Stohlman, F. (Ed.), Hemopoietic Cellular Proliferation. Grune & Stratton, New York, pp. 3–14.

Morley, A., Stohlman, F., 1970. Cyclophosphamide induced cyclical neutropenia. N. Engl. J. Med. 282, 643–646.

Nakamura, M., 1999. Estimation of cell cycle parameters from cell division tracking data. Master's Thesis, University of New South Wales.

Niu, L., Golde, D.W., Vera, J.C., Heaney, M.L., 1999. Kinetic resolution of two mechanisms for high-affinity granulocyte-macrophage colony-stimulating factor binding to its receptor. Blood 94, 3748–3753.

Novak, J.P., Nečas, E., 1994. Proliferation differentiation pathways of murine haematopoiesis: correlation of lineage fluxes. Cell Prolif. 27, 597–633.

Oostendorp, R.A., Audet, J., Eaves, C.J., 2000. High-resolution tracking of cell division suggests similar cell cycle kinetics of hematopoietic stem cells stimulated in vitro and in vivo. Blood 95, 855–862.

Petros, W., 1992. Pharmacokinetics and administration of colony-stimulating factors. Pharmacotherapy 12, 32S–38S.

Price, T.H., Chatta, G.S., Dale, D.C., 1996. Effect of recombinant granulocyte colony stimulating factor on neutrophil kinetics in normal young and elderly humans. Blood 88, 335–340.

Reeve, J., 1973. An analogue model of granulopoiesis for the analysis of isotopic and other data obtained in the non-steady state. Br. J. Haematol. 25, 15–32.

Rubinow, S.I., Lebowitz, J.L., 1975. A mathematical model of neutrophil production and control in normal man. J. Math. Biol. 1, 187–225.

Santillan, M., Bélair, J., Mahaffy, J.M., Mackey, M.C., 2000. Regulation of platelet production: the normal response to perturbation and cyclical platelet disease. J. Theor. Biol. 206, 585–903.

Schmitz, S., Franke, H., Loeffler, M., Wichmann, H.E., Diehl, V., 1994. Reduced variance of bone-marrow transit time of granulopoiesis: a possible pathomechanism of human cyclic neutropenia. Cell Prolif. 27, 655–667.

Schmitz, S., Franke, H., Wichmann, H.E., Diehl, V., 1995. The effect of continuous G-CSF application in human cyclic neutropenia: a model analysis. Br. J. Haematol. 90, 41–47.

Schmitz, S., Loeffler, M., Jones, J.B., Lange, R.D., Wichmann, H.E., 1990. Synchrony of bone marrow proliferation and maturation as the origin of cyclic haemopoiesis. Cell Tissue Kinet. 23, 425–441.

Shvitra, D., Laugalys, R., Kolesov, Y.S., 1983. Mathematical modeling of the production of white blood cells. In: Marchuk, G., Belykh, L. (Eds.), Mathematical Modeling in Immunology and Medicine. North-Holland, Amsterdam, pp. 211–223.

Stefanich, E., Senn, T., Widmer, R., Fratino, C., Keller, G.-A., Fielder, P.J., 1997. Metabolism of thrombopoietin (TPO) in vivo: determination of the binding dynamics for TPO in mice. Blood 89, 4063–4070.

Takatani, H., Soda, H., Fukuda, M., Watanabe, M., Kinoshita, A., Nakamura, T., Oka, M., 1996. Levels of recombinant human granulocyte colony-stimulating factor in serum are inversely correlated with circulating neutrophil counts. Antimicrob. Agents Chemother. 40, 988–991.

Terashi, K., Oka, M., Ohdo, S., Furukubo, T., Ikeda, C., Fukuda, M., Soda, H., Higuchi, S., Kohno, S., 1999. Close association between clearance of recombinant human granulocyte colony-stimulating factor (G-CSF) and G-CSF receptor on neutrophils in cancer patients. Antimicrob. Agents Chemother. 43, 21–24.

Vickers, M., Brown, G.C., Cologne, J.B., Kyoizumi, S., 2000. Modelling haemopoietic stem cell division by analysis of mutant red cells. Br. J. Haematol. 110, 54–62.

von Schulthess, G.K., Mazer, N.A., 1982. Cyclic neutropenia (CN): a clue to the control of granulopoiesis. Blood 59, 27–37.

Ward, A.C., van Aesch, Y.M., Gits, J., Schelen, A.M., de Koning, J.P., van Leeuwen, D., Freedman, M.H., Touw, I.P., 1999. Novel point mutation in the extracellular domain of the granulocyte colony-stimulating factor (G-CSF) receptor in a case of severe congenital neutropenia hyporesponsive to G-CSF treatment. J. Exp. Med. 190, 497–508.

Weinblatt, M.E., Scimeca, P., James-Herry, A., Sahdev, I., Kochen, J., 1995. Transformation of congenital neutropenia into monosomy 7 and acute nonlymphoblastic leukemia in a child treated with granulocyte colony-stimulating factor. J. Pediatr. 126, 263–2655.

Wichmann, H.E., Loeffler, M., Schmitz, S., 1988. A concept of hemopoietic regulation and its biomathematical realization. Blood Cells 14, 411–429.

Williams, G., Smith, C., Spooncer, E., Dexter, T., Taylor, D., 1990. Haemopoietic colony stimulating factors promote cell survival by suppressing apoptosis. Nature 343, 76–79.

Wright, D.G., Dale, D.C., Fauci, A.S., Wolff, S.M., 1981. Human cyclic neutropenia: clinical review and long term follow up of patients. Medicine 60, 1–13.